19. Leskinen-Kallio S, Ruotsalainen U, Någren K, Teräs M, Joensuu H. Uptake of carbon-11-methionine and fluorodeoxyglucose in non-Hodgkin's lymphoma: a PET study. *J Nucl Med* 1991;32:1211–1218.
20. Kern KA, Brunetti A, Norton JA, et al. Metabolic imaging of human extremity musculoskeletal tumors by PET. *J Nucl Med* 1988;29:181–186.
21. Haberkorn U, Strauss LG, Reisser CH, et al. Glucose uptake, perfusion, and cell proliferation in head and neck tumors: relation of positron emission tomography to flow cytometry. *J Nucl Med* 1991;32:1548–1555.
22. Olefsky JM. Obesity. In: Wilson JD, Braunwald E, Isselbacher KJ, eds. *Harrison's principles of internal medicine, volume 1*, 12th edition. New York: McGraw-Hill; 1991:411.
23. UICC. International union against cancer. *TNM classification of malignant tumours*, 4th edition. Geneva: 1987.
24. Hamacher K, Coenen HH, Stöcklin G. Efficient stereospecific synthesis of no-carrier-added 2-[^{18}F]-Fluoro-2-Deoxy-D-Glucose using aminopolyether supported nucleophilic substitution. *J Nucl Med* 1986;27:235–238.
25. Patlak CS, Blasberg RG, Fenstermacher JD. Graphical evaluation of blood-to-brain transfer constants from multiple-time uptake data. *J Cereb Blood Flow Metab* 1983;3:1–7.
26. Reivich M, Alavi A, Wolf A, et al. Glucose metabolic rate kinetic model parameter determination in humans: the lumped constants and rate constants for [^{18}F]fluorodeoxyglucose and [^{11}C]deoxyglucose. *J Cereb Blood Flow Metab* 1985;5:179–192.
27. Fidler I. The biology of human cancer metastasis. *Acta Oncol* 1991;6: 669–675.
28. Herholz K, Ziffling P, Staffen W, et al. Uncoupling of hexose transport and phosphorylation in human gliomas demonstrated by PET. *Eur J Cancer Clin Oncol* 1988;7:1139–1150.
29. Lammertsma AA, Brooks DJ, Frackowiak RSJ, et al. Measurement of glucose utilization with [^{18}F]2-fluoro-2-deoxy-D-glucose: a comparison of different analytical methods. *J Cereb Blood Flow Metab* 1987;7:161–172.
30. Herholz K, Wienhard K, Heiss W-D. Validity of PET studies in brain tumors. *Cereb Brain Metab Rev* 1990;2:240–265.
31. Spence AM, Graham MM, Munzi M, et al. Assessment of glucose metabolism in malignant gliomas: use of deoxyglucose or glucose [Abstract]. *Second European Workshop on FDG in Oncology*. Heidelberg, 1991.

EDITORIAL

FDG-PET in Oncology: There's More to It Than Looking at Pictures

"Things sweet to taste may prove in digestion sour."
William Shakespeare

Rapidly proliferating tumor cells metabolize glucose more rapidly under anerobic than under aerobic conditions. This inhibition of glycolysis by oxygen, the "Pasteur effect," was first described by Pasteur and later confirmed by Warburg and Meyerhof (*1,2*). Proposed explanations for this phenomenon include, increased concentrations of hexokinase in tumors compared to normal tissue and increased glucose transport into tumors (*3–5*). Accelerated glucose transport is among the most characteristic biochemical changes that occur with cellular transformation. In a recent study, the molecular mechanism of altered glucose transporter activity was evaluated in cultured rat fibroblasts transfected with activated myc, ras and src oncogenes (*6,7*). In cells transfected with myc, the rate of 2-deoxy-D-glucose transport was unchanged. In contrast, transfection with ras and src oncogenes resulted in dramatically increased glucose transport which was paralleled by marked increases in the amounts of glucose transporter protein and messenger RNA. Similarly, exposure of the cells to the tumor promoting phorbol ester 12-O-tetradecanoyl phorbol-13-acetate also resulted in accelerated glucose transport and increased concentrations of transporter mRNA. These results indicate that a significant mechanism by which malignant transformation activates glucose transport is increased expression of the structural gene encoding the glucose transport protein.

The ex vivo evaluation of glucose metabolism in tumors can be performed with ^{3}H or ^{14}C-labeled glucose. However, the fact that glucose is extensively metabolized in vivo requires detailed chromatographic analysis of the concentration of individual metabolites. The introduction of radiolabeled 2-deoxy-D-glucose by Sokoloff et al. as a tracer of glucose metabolism has greatly facilitated these measurements (*8*). Since this tracer lacks a hydroxyl group in the 2 position, the first glucose metabolite, 2-deoxy-D-glucose-6-PO_4, is not a substrate for glucose-phosphate isomerase and cannot be converted to fructose-6-PO_4. For similar reasons, 2-deoxy-D-glucose cannot be converted to glycogen. Thus, the formation of 2-deoxy-D-glucose-6-PO_4, is the final step in the absence of glucose-6-phosphatase, which catalyzes the reverse reaction to 2-deoxy-D-glucose. Since it is highly negatively charged, 2-deoxy-D-glucose-6-PO_4 accumulates intracellularly. Due to the isoteric relationship between hydrogen and fluorine, the positron emitting glucose analog 2-[^{18}F]fluoro-2-deoxy-D-glucose (FDG) can be used for the in vivo measurement of glucose metabolism in humans by PET.

Following injection, FDG is transported into the cells of most tissues by facilitated diffusion, phosphorylated to FDG-6-PO_4 and trapped intracellularly (*8–11*). Thus, the annihilation photons of ^{18}F that are detected by PET originate from FDG in plasma and tissue and intracellular FDG-6-PO_4. Within 1 hr after injection, most of the radiation emitted from tissues with low concentrations of glucose-6-phosphatase, such as heart, brain and many tumors, comes from intracellular FDG-6-PO_4. Tissues with high levels of this enzyme, such as liver, kidney, intestine and muscle, accumulate small amounts of FDG-6-PO_4 and contribute a low level of background radioactivity to PET images.

Received Sept. 21, 1992; accepted Sept. 21, 1992.

For correspondence or reprints contact: Dr. Alan J. Fischman, Division of Nuclear Medicine, Department of Radiology, Massachusetts General Hospital, 32 Fruit St., Boston, MA 02114.

When plateau concentrations of FDG are achieved in tissues with low concentration of glucose-6-phosphatase, images of total ^{18}F radioactivity reflect relative rates of glycolysis. At earlier times, knowledge of the rate constants of the FDG model is required to interpret imaging data in terms of glycolytic rates. These rate constants have been determined for normal brain and heart, and it has been demonstrated that reliable data can be acquired at $\geq$ 45 min after injection. Since similar data are not available for most tumors, appropriate imaging times have not as yet been defined.

At steady-state, in tissues with low levels of glucose-6-phosphatase activity, the transport of FDG can be described by the relatively simple three-compartment Sokoloff model. In the absence of significant glucose-6-phosphatase activity, the concentration of FDG in tissue will eventually reach a plateau. The plateau concentration (C_T) represents the metabolically trapped ^{18}F label. The total availability of FDG to tissue is given by the product of local blood flow (F) and the area (A) under the arterial plasma curve. Thus, the product of local blood flow (ml/min/g) and net capillary extraction of FDG (E_n) is the ratio of C_T-to-A:

$$F \cdot E_n - C_T/A.$$

By the Fick principle, the glucose utilization rate is:

$$F \cdot E_{11} \cdot [Glu]/LC - (C_T/A) \cdot [Glu]/LC,$$

where [Glu] is the plasma glucose concentration and LC is the so-called "lumped constant," equivalent to the ratio of net extraction of natural glucose to the net extraction of FDG. It should be noted that this expression is independent of any detailed compartmental model and does not specifically require knowledge of model rate constants. Prior to the plateau, calculation of metabolic rate is model-dependent, requiring assumptions about capillary bed geometry, trans-capillary transport, compartmentation at the cellular level and dynamic measurements of tissue and plasma FDG concentrations.

The evaluation of glucose metabolism from FDG images can be performed at four levels of sophistication:

1. Qualitative inspection of static images acquired after FDG reaches plateau concentration. This technique is useful for the identification of focal areas of high FDG accumulation that are characteristic of aggressive tumors and is the most commonly used technique in clinical practice.
2. Semiquantitative analysis of plateau images based on: (a) relative lesion radioactivity normalized to injected dose and body weight (SUV, DUR) or (b) region of interest (ROI) ratios.
3. Quantitative measurement of the local glucose metabolic rate, MRGlc (μmol/100 g/min), from images acquired at a single time with a priori estimates of the rate constants.
4. Quantitative measurement of the local glucose utilization rate, MRGlc, with independent measurement of k_1-k_3. For this measurement, a dynamic imaging sequence with simultaneous arterial blood sampling is used and the model rate constants are estimated by fitting the tissue and plasma FDG concentration data to a compartmental model.

Although the Sokoloff model is relatively insensitive to the rate constants, k_1-k_3 are not universal constants and reflect ambient steady-state conditions of transport and phosphorylation. Since method 3 relies on an a priori knowledge of the rate constants in the model, it is generally not applicable to measurements of glucose metabolism in tumors for which population estimates of these parameters are not available and a dynamic study must be performed (method 4). Currently, values for these rate constants are only available for some tumors of the CNS.

Even when dynamic PET data is available, conversion of FDG data to glucose metabolic rates relies on the value of the lumped constant. The LC is composed of six individual terms:

$$LC = (K_m/V_{max})_{Gn} \cdot (V_{max}/K_m)_{FDG} \cdot \left(\frac{\lambda}{\phi}\right),$$

where K_m and V_{max} are the Michaelis-Menton parameter for glucose and FDG, λ is the ratio of the distribution volumes of FDG and glucose ϕ is a measure of the amount of glucose-6-phosphate that undergoes further metabolism. It is defined as (1-r/v), where r is the rate of glucose-6-phosphate hydrolysis and v is the rate glucose phosphorylation by hexokinase).

The value of the lumped constant is highly dependent on the physiological conditions that prevail during the measurement. In general, major changes in the lumped constant occur whenever glucose utilization becomes supply limited (*12*). A change in any of the six parameters that contribute to the lumped constant could significantly alter its value.

Although the number of studies comparing the Michaelis-Menton parameters for glucose and FDG in tumors has been limited, the importance of this contribution to the lumped constant has been considered. For example, in a study of transplantable rat gliomas, it was shown that the K_m for glucose in tumors was significantly greater ($p < 0.02$) than in normal brain, however, the K_m for 2-deoxyglucose was similar in tumors and normal brain (*13,14*). In tumors, the K_m for 2-deoxyglucose was greater than for glucose. In contrast, the value for V_{max} was relatively constant for glucose and 2-deoxyglucose in both normal brain and tumor. From these data, it was determined that the lumped constant is increased 2.26-fold in intracerebral glioma compared to normal brain.

Changes in lambda and phi can also affect the lumped constant (*15–17*). Under pathological conditions, tissue damage can alter normal cellular compartmentation and it cannot be

assumed that the ratio of distribution volumes for glucose and FDG remains constant. For example, in stroke, alterations in distribution volume ratio have been shown to influence the lumped constant more than any other factor (*16*). Also, in pathological tissue (particularly when a significant degree of necrosis is present), release of lysosomal acid hydrolases can occur and these enzymes can hydrolyze glucose-6-phosphate and affect phi.

Considering the number of sources for variability in the lumped constant, it is clear that the interpretation of FDG data from any type of tumor must proceed with extreme caution. This is particularly important for the interpretation of serial studies performed during a course of chemo- or radiation therapy. In fact, it is possible that under some circumstances changes in the lumped constant could completely mask the effect of changes in rate constants on glucose utilization rate.

Although the lumped constant has been measured for some types of CNS tumors, values for other types of tumor are totally lacking. To obtain this information, experiments in animals must be performed with each specific type of tumor being evaluated.

Currently, it is well established that FDG-PET imaging of primary brain tumors is a useful procedure for: noninvasive grading of gliomas, monitoring tumor progression and evaluating response to therapy (i.e., differentiation of radiation necrosis from tumor recurrence). FDG-PET has been used to evaluate other types of tumors, including lung carcinoma (*18–21*), head and neck tumors (*22–25*), lymphoma (*26–30*), musculoskeletal tumors (*31–33*), breast carcinoma (*34–38*), colorectal carcinoma (*39,40*), liver tumors (*41*) and thyroid tumors (*42*). However, with a few exceptions (*41*), the necessary metabolite basis for interpreting the imaging data is far less developed than for CNS malignancies. In most cases, the interpretation of PET images from these tumors has relied on extrapolations from the results of studies of primary brain tumors.

Although to a first approximation, FDG-PET can be used for the detection of malignant tissue, a definitive evaluation of FDG images demands a relatively high degree of metabolic sophistication in the observer. Under no circumstances should FDG be treated as a "contrast agent." Similarly, the mechanism of FDG accumulation is significantly more complex than the other radiopharmaceuticals used in nuclear medicine, such as sulfur colloid, gallium citrate or MDP. Only by considering the imaging data in the context of the overall metabolic status of the patient can the required level of insight be achieved. In many ways, the interpretation of an FDG study is similar to the appreciation of a work of art or a piece of music. When viewing a work of Picasso, even a relative novice can discern the colors and shapes, however, the eye of a true connoisseur is required to appreciate the full meaning of the work. Similarly, although someone unschooled in music theory can enjoy a Mozart concerto, only individuals with the appropriate technical training can appreciate the underlying patterns in the piece.

In this issue of the *Journal*, Lindholm et al. (*43*) evaluated the effect of blood glucose concentration on FDG uptake in five patients with squamous cell carcinoma of the head and neck (tongue, 2 patients; hypopharynx with neck metastasis, 1 patient; lip with neck metastasis, 1 patient; larynx with neck metastasis, 1 patient). Using a 60-min dynamic acquisition, they determined SUVs and Patlak K_i values (*44*) for regions of interest drawn on "hot spots" of tumorous and normal tissue. In each patient, the study was performed under both fasting and glucose loaded conditions. In the fasting study, plasma glucose and insulin levels were measured at the time of FDG injection and the plasma glucose measurements were repeated 30 and 60 min later. In the glucose loaded study, plasma glucose and insulin levels were measured at −60, −30, 0, 30 and 60 min. The FDG metabolic rate was determined by multiplying K_i by the average plasma glucose concentration during scanning. The lumped constant was assumed to be one. Also the metabolic index for FDG was calculated by multiplying the SUV by the average plasma glucose concentration. The SUVs and K_is were compared by linear regression. The fasting SUVs of the tumors ranged from 4.1 to 10.9, and after glucose loading the values decreased significantly, ranging from 2.2 to 5.9. The fasting K_is of the tumors ranged from 0.021 to 0.067, and after glucose loading the values decreased significantly, 0.006–0.042. The overall correlation between SUV and K_i was excellent. The SUVs for the cerebellum also decreased with glucose loading. In contrast, the SUVs for normal tongue and neck muscle increased with glucose loading. The metabolic index of FDG of the tumors increased by 10% with glucose loading, while the FDG metabolic rate increased by 36%. The increase in FDG uptake in normal muscle explains the blurring of the PET images that were recorded under glucose loaded conditions. Based on these results, the authors correctly conclude that plasma glucose concentration should always be considered when grading or staging tumors or trying to correlate a change in FDG uptake with treatment response.

Overall, this work represents an important contribution to the PET-oncology literature. However, several aspects of the discussion have been significantly oversimplified and do not adequately reflect the importance of a detailed understanding of the overall metabolic state of the tissues being studied on FDG accumulation. For example, an important consideration when quantitating studies with glucose loading is the effect of nonsteady-state conditions. This is a key assumption in the Sokoloff model. If steady-state does not prevail, the k's are no longer constant. Unfortunately, this issue is not discussed.

In the present study, there is no indication of possible explanations for

the divergent effects of glucose loading on SUVs and K_is for neoplastic and normal tissues. These differences could be explained by difference in the degree of saturation of glucose transporters in the different tissues and differential sensitivity to insulin. If it is assumed that the glucose transporters of the tumors are saturated at fasting glucose concentrations, further increasing the plasma glucose concentration should inhibit FDG transport. Also, since it is well established that glucose transport into muscle is highly insulin-dependent, the measured 6.7–15.7-fold increase in peak insulin level induced by glucose loading could explain the increases in SUV and K_i. However, even this explanation could represent an oversimplification since after glucose is transported into muscle it is phosphorylated to glucose-6-phosphate which can then inhibit hexokinase by an allosteric mechanism. In this way, it is effectively competing with ATP and the net inhibitory effect depends on the ratio of glucose-6-phosphate to ATP and thus the energy state of the muscle. Thus, since the background tissue for all the tumors studied in this investigation was muscle, the decrease in tumor definition with glucose loading can be readily explained. For tumors with normal livers as background, hyperglycemia should also blur tumor margins, however, the explanation for this effect is different. Since insulin is secreted by the pancreas, the liver is exposed to much higher concentrations of insulin than other tissues. However, unlike other peripheral tissues, liver cells are freely permeable to glucose and hepatic glucose transport is not sensitive to insulin. Also, hepatic glucose phosphorylation is catalyzed by both hexokinase and a unique enzyme, glucokinase. Glucokinase has a 100-fold higher K_m than hexokinase, is inducible by insulin and is not allosterically inhibited by glucose-6-phosphate. In addition, insulin inhibits the enzyme glucose-6-phosphatase, the final reaction of gluconeogenesis. Thus, with glucose loading, FDG phosphorylation is increased and dephosphorylation is decreased, leading to a net increase in FDG-6-P trapping and increased background activity. When tumors are located in other insulin-sensitive tissues, such as bone, mammary gland, pituitary and peripheral nerves, similar effects of glucose loading on background FDG accumulation might be observed. In contrast, for insulin-insensitive tissues, such as the brain and the gonads, the effect of glucose loading on tumor to normal tissue FDG accumulation is more dependent on the relative number and saturation of glucose transporters. To develop a quantitative understanding of FDG metabolism in oncology, it will be necessary to determine the number and affinity of glucose transporters in a variety of different types of tumors. These measurements can be performed by serial dynamic FDG studies under experimental conditions in which plasma glucose levels are clamped at predetermined values.

In contrast to the results reported by Lindholm et al., it is possible that in some situations glucose loading will lead to improved tumor definition. Recently, we observed this effect in an FDG-PET study of a patient with a pituitary tumor. In spite of instructions to fast before the study, this subject had lunch 2 hr before injection of the FDG. Although FDG accumulation in the brain was markedly decreased, accumulation of radioactivity in the tumor was excellent (Fig. 1). Approximately 1 wk later, the subject was restudied under the usual fasting condition. In the second examination, accumulation of FDG in the brain was greater but the level of radioactivity in the tumor was lower. The better tumor-to-brain definition in the first study was probably due to inhibition of FDG uptake in the brain by glucose and insulin stimulated FDG uptake by the pituitary.

Another issue that was not considered by Lindholm et al. is the time at which SUVs were determined. The imaging protocol used was probably adapted from FDG imaging of the brain and there was no indication that

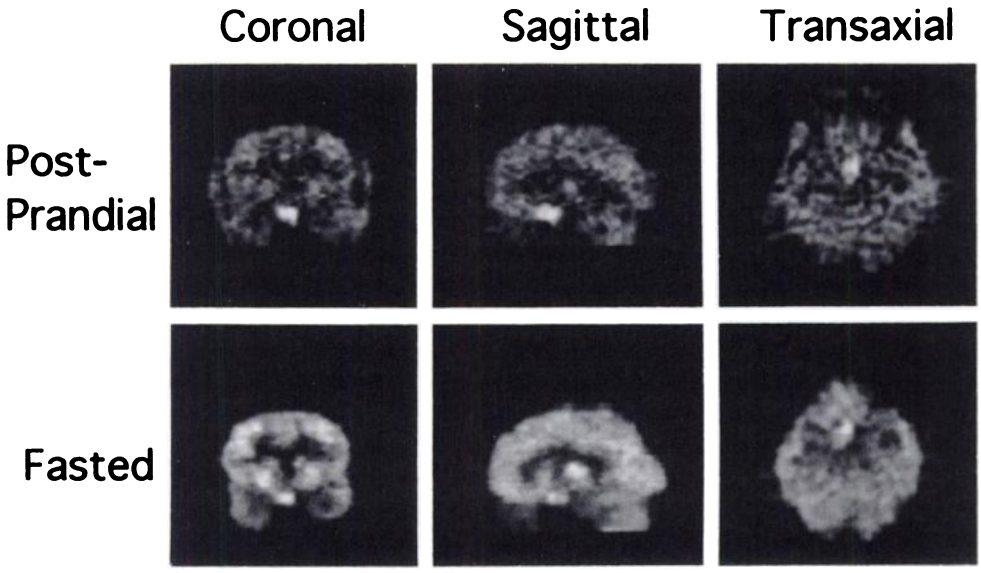

FIGURE 1. Representative coronal, sagittal and transaxial FDG images from a patient with a pituitary tumor. The upper images were acquired within two hours after the patient had eaten. The lower images were acquired in the fasting state. In both studies, the patient was injected with ~10 mCi of FDG and imaging was performed 60 min later. The images were normalized to injected dose, imaging time and body weight.

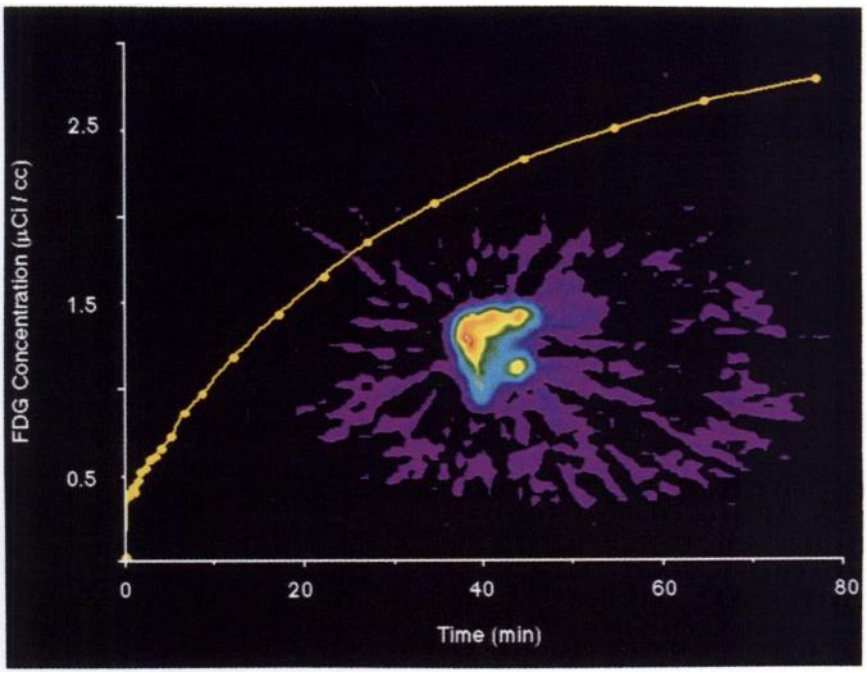

FIGURE 2. Representative transaxial FDG image and time-activity curve from a patient with non-small cell carcinoma of the lung. After an overnight fast, the subject was injected with ~10 mCi of FDG and serial PET images were acquired over 90 min. The displayed image was acquired at 90 min postinjection.

the tumors achieved plateau concentration within 60 min. If the level of FDG accumulation is changing at the time the SUV is measured, significant errors in interpretation can be made. This issue is of particular importance in busy clinical PET centers where several patients may be injected with FDG at the same time and are imaged when scanner time becomes available. Recently, this problem occurred at our institution. In the course of developing a clinical protocol for FDG-PET imaging of non-small cell lung tumors, we performed dynamic PET imaging in a series of patients to determine the time for optimal imaging. Figure 2 shows a decay-corrected time-activity curve for one of the subjects. From this data, it is clear that even at 90 min after injection of FDG, plateau concentrations of radioactivity are not achieved. Similar results were obtained for most of the patients that were studied. These results prompted us to take particular care in evaluating nondynamic studies by the SUV method. These results emphasize that the FDG kinetics of every type of tumor to be studied clinically must be well understood for meaningful results to be obtained.

The use of FDG for the qualitative and quantitative evaluation of tumor metabolism is currently the fastest growing arena of clinical PET. However, it is important to remember that Sokoloff and colleagues spent many years establishing the validity of the deoxyglucose method under a very narrow set of conditions: brain tissue, steady-state and a specific species. Haphazard extrapolations of the method to pathophysiological conditions are almost certain to lead to confusing and inconsistent results, a situation that will reflect badly on the field of nuclear medicine. With FDG-PET, fundamental aspects of tumor biology can be applied to clinical diagnosis. However, only by considering each type of tumor individually and in the metabolic context of the patient can meaningful results be obtained.

Alan J. Fischman
Nathaniel M. Alpert
Massachusetts General Hospital,
Boston, Massachusetts
Harvard Medical School
Boston, Massachusetts

REFERENCES

1. Warburg O. *The metabolism of tumors.* New York, Richard R. Smith, Inc.; 1931:129-169.
2. Warburg O. On the origin of cancer cells. *Science* 1956;123:309–314.
3. Weber G, Banaejee G, Morris HP. Comparative chemistry of hepatomas. 1. Carbohydrate enzymes in morris hepatomas 5123. *Cancer Res* 1961;21:933–937.
4. Monakhov NK, Neistadt EL, Shavlovskii MM, et al. Physicochemical properties and isoenzyme composition of hexokinase from normal and malignant human tissues. *J Natl Cancer Inst.* 1978;61:27–34.
5. Hatanaka M, Augl C, Gilden RV. Evidence for a functional chain in the plasma membrane of murine sarcoma virus-infected mouse embryo cells. Transport and transport associated phosphorylation of ^{14}C-2-deoxy-D-glucose. *J Biol Chem* 1970;245:714–717.
6. Flier JS, Mueckler MM, Usher P, Lodish HF. Elevated levels of glucose transport and transporter messenger RNA are induced by ras and sarc oncogenes. *Science* 1987;235:1492–1495.
7. Birnbaum MJ, Haspel HC, Rosen OM. Transformation of rat fibroblasts by FSV rapidly increases glucose transporter gene transcription. *Science* 1987;235:1495–1498.
8. Sokoloff L, Reivich M, Kennedy C, et al. The ^{14}C-deoxyglucose method for the measurement of local cerebral glucose utilization: theory, procedure and normal values in the conscious and anesthetized albino rat. *J Neurochem* 1977;28: 897–916.
9. Phelps ME, Huang SC, Hoffman EJ, et al. Tomographic measurements of local cerebral glucose metabolism in humans with (F-18)-2-fluoro-2-deoxy-D-glucose: validation of method. *Ann Neurol* 1979;6:371–388.
10. Horton RW, Meldrum BS, Bachelard HS. Enzymatic and cerebral metabolic effects of 2-deoxy-D-glucose. *J Neurochem* 1973;21: 506–520.
11. Som P, Atkins HL, Bandoypadhyay D, et al. A fluorinated glucose analog, 2-fluoro-2-deoxy-D-glucose (^{18}F): nontoxic tracer for rapid tumor detection. *J Nucl Med* 1980;21:670–675.
12. Crane PD, Partridge WM, Braun LD, et al. The

interaction of transport and metabolism on brain glucose utilization: a re-evaluation of the lumped constant. *J Neurochem* 1981;36: 1601–1604.
13. Kapoor R, Spence AM, Muzi M, et al. Determination of the deoxyglucose and glucose phosphorylation ratio and the lumped constant in rat brain and a transplantable rat glioma. *J Neurochem* 1989;53:37–44.
14. Spence AM, Graham MM, Muzi M, et al. Deoxyglucose lumped constant estimated in a transplanted rat astrocytic glioma by the hexose utilization index. *J Cereb Blood Flow Metab* 1990;10:190–198.
15. Gedda A, Diksik M, Yamamoto YL, Feindel W. Comparative regional analysis of 2-deoxyglucose and methylglucose uptake in brain of four stroke patients. With special reference to the regional estimation of the lumped constant. *J Cereb Blood Flow Metab* 1985;5:163–178.
16. Nakai H, Matsuda H, Takara E, et al. Simultaneous in vivo measurement of lumped constant and rate constants in experimental cerebral ischemia using F-18 FDG. *Stroke* 1987; 18:158–167.
17. Nakai H, Yamamoto YL, Diksic M, et al. Time-dependent changes of lumped and rate constants in the deoxyglucose method in experimental cerebral ischemia. *J Cereb Blood Flow Metab* 1987;7:640–648.
18. Nolop KB, Rhodes CG, Brudin LH, et al. Glucose utilization in vivo by human pulmonary neoplasms. *Cancer* 1987;60:2682–2689.
19. Abe Y, Matsuzawa T, Fujiwara T, et al. Clinical assessment of therapeutic effects on cancer using ^{18}F-2-fluoro-2-deoxy-D-glucose and positron emission tomography: preliminary study of lung cancer. *Int J Radiat Oncol Biol Phys* 1990;19:1005–1010.
20. Ichiya Y, Kuwabara Y, Otsuka M, et al. Assessment of response to cancer therapy using fluorine-18-fluorodeoxyglucose and positron emission tomography. *J Nucl Med* 1991;32: 1655–1660.
21. Gupta NC, Frank AR, Dewan NA, et al. Solitary pulmonary nodules: detection of malignancy with PET with 2-[F-18]-fluoro-2-deoxy-D-glucose. *Radiology* 1992;184:441–444.
22. Minn H, Joensuu H, Ahonen A, Klemi P. Fluorodeoxyglucose imaging: a comparison with DNA flow cytometry in head and neck tumors. *Cancer* 1988;61:1776–1781.
23. Chen BC, Hoh C, Choi Y, et al. Evaluation of primary head and neck tumors with PET FDG [Abstract]. *Clin Nucl Med* 1990;15:758.
24. Haberkorn U, Strauss LG, Reisser C, et al. Glucose uptake, perfusion, and cell proliferation in head and neck tumors: relation of positron emission tomography to flow cytometry. *J Nucl Med* 1991;32:1548–1555.
25. Bailet JW, Abemayor E, Jabour BA, et al. Positron emission tomography: a new, precise imaging modality for detection of primary head and neck tumors and assessment of cervical adenopathy. *Laryngoscope* 1992;102:281–288.
26. Paul R. Comparison of fluorine-18-2-fluorodeoxyglucose and gallium-67-citrate imaging for the detection of lymphoma. *J Nucl Med* 1987;28:288–292.
27. Okada J, Yoshikawa K, Itami M, et al. Positron emission tomography using fluorine-18-fluorodeoxyglucose in malignant lymphoma: a comparison with proliferative activity. *J Nucl Med* 1992;33:325–329.
28. Okada J, Yoshikawa K, Imazeki K, et al. The use of FDG-PET in the detection and management of malignant lymphoma: correlation of uptake with prognosis. *J Nucl Med* 1991;32: 686–691.
29. Kubota K, Yamada K, Yoshioka S, et al. Differential diagnosis of idiopathic fibrosis from malignant lymphadenopathy with PET and F-18 fluorodeoxyglucose. *Clin Nucl Med* 1992; 17:361–363.
30. Kuwabara Y, Ichiya Y, Otsuka M, et al. High [^{18}F]FDG uptake in primary cerebral lymphoma: a PET study. *J Comput Assist Tomogr* 1988;12:47–48.
31. Kern KA, Brunetti A, Norton JA, et al. Metabolic imaging of human extremity musculoskeletal tumors by PET. *J Nucl Med* 1988;29: 181–186.
32. Adler LP, Blair HF, Makley JT, et al. Noninvasive grading of musculoskeletal tumors using PET. *J Nucl Med* 1991;32:1508–1512.
33. Kern KA, Brunetti A, Norton JA, et al. Metabolic imaging of human extremity musculoskeletal tumors by PET. *J Nucl Med* 1988;29: 181–186.
34. Hoh C, Hawkins RA, Glaspy J, et al. PET total body imaging in breast cancer with F-18 ion and FDG [Abstract]. *Clin Nucl Med* 1990;15: 763.
35. Wahl RL, Cody R, Hutchins G, Mudgett E, et al. Positron emission tomographic scanning of primary and metastatic breast carcinoma with the radiolabeled glucose analog 2-deoxy-2[^{18}F] fluoro-D-glucose. *N Engl J Med* 1991;324: 200.
36. Tse NY, Hoh CK, Hawkins RA, et al. The application of positron emission tomographic imaging with fluorodeoxyglucose to the evaluation of breast disease. *Ann Surg* 1992;216: 27–34.
37. Wahl RL, Cody RL, Hutchins GD, Mudgett EE. Primary and metastatic breast carcinoma: initial clinical evaluation with PET with the radiolabeled glucose analogue 2-[F-18]-fluoro-2-deoxy-D-glucose. *Radiology* 1991;179: 765–770.
38. Kubota K, Matsuzawa T, Amemiya A, et al. Imaging of breast cancer with [^{18}F]fluorodeoxyglucose and positron emission tomography. *J Comput Assist Tomogr* 1989;13:1097–1098.
39. Yonekura Y, Benua RS, Brill AB, et al. Increased accumulation of 2-deoxy-2[^{18}F]fluoro-D-glucose in liver metastases from colon carcinoma. *J Nucl Med* 1982;23:1133–1137.
40. Strauss LG, Clorius JH, Schlag P, et al. Recurrence of colorectal tumors: PET evaluation. *Radiology* 1989;170:329–332.
41. Okazumi S, Isono K, Enomoto K, et al. Evaluation of liver tumors using fluorine-18-fluorodeoxyglucose PET: characterization of tumor and assessment of effect of treatment. *J Nucl Med* 1992;33:333–339.
42. Joensuu H, Ahonen A. Imaging of metastases of thyroid carcinoma with fluorine-18 fluorodeoxyglucose. *J Nucl Med* 1987;28:910–914.
43. Lindholm P, Minn H, Leskinen-Kallio S, et al. Influence of the blood glucose concentration on FDG uptake in cancer—a PET study. *J Nucl Med* 1993;34:1–6.
44. Patlak CS, Blasberg RG, Fenstermacher JD. Graphical evaluation of blood-to-brain transfer constants form multiple-time uptake data. *J Cereb Blood Flow Metab* 1983;3:1–7.